The Astrophysical Journal, 491:242–253, 1997 December 10

THE HIGH-EXCITATION PLANETARY NEBULA NGC 7662

Siek Hyung
Bohyunsan Optical Astronomy Observatory, Jachun P.O. Box 1, Youngcheon, Kyungbuk 770-820, Korea; hyung@astro.ucla.edu, hyung@hanul.issa.re.kr

and

Lawrence H. Aller
Physics and Astronomy Department, University of California, Los Angeles, CA 90095; aller@bonnie.astro.ucla.edu
Received 1997 June 3; accepted 1997 July 24

ABSTRACT

Wavelengths and identifications have been provided for approximately 300 lines between 3660 and 10125 Å in the spectrum of the archetypal bright, high-excitation planetary nebula NGC 7662. These lines are measured with the Hamilton echelle spectrograph at Lick Observatory and are supplemented by image-tube data. Published results are used to construct diagnostic diagrams and derive ionic concentrations. The electron temperature indicated by [O III] is about 12,500 K; the density regimes consist of $N_\epsilon = 5000$–17,000 cm^{-1}. Derivation of precise abundances will require appropriate model calculations, but with the aid of homogeneous spherical model procedures we find C to be enhanced, N marginally so if at all, and heavier elements depleted with respect to the Sun. These conclusions are in harmony with those of Barker.

Subject headings: ISM: abundances — line: identification — planetary nebulae: individual (NGC 7662)

1. INTRODUCTION

Because of its favorable position for Northern Hemisphere observers and its brightness, high excitation, and rich spectrum, NGC 7662, PK 106−17°1, has been a favorite object for observers. Actually, it is really a triple shell structure involving the following components: a bright, inner ring; a fainter outer one familiar to all students of planetary nebulae (PNs); and a nearly circular, extremely dim uniform halo. This outer halo of 72″ has a mass of about 0.19 $M_\odot$ and is nearly 20,000 times fainter than the bright ring (Middlemass et al. 1991). The electron temperature, T_ϵ, of the halo as measured by the [O II] lines is 17,500 K, some 4400 K hotter than the core. The material of the halo is heated by the brisk winds blowing through the PN, only a small fraction of whose energy is needed to excite the lines. To add to our appreciation of the complexity of PNs such as NGC 7662, we mention the small blobs known as FLIERS (fast-moving, low-ionization, and emission regions that show no Ne^{++}, O^{++}, etc., with dynamical ages of ∼1000 yr). They appear in most PNs as pairs, moving with equal and opposite velocities, typically ∼50 km s^{-1}. The masses are 10^{-4}–10^{-5} that of the Sun, but they show little difference in temperature and density from their environments, which appear to be much older (see Balick 1987; Balick et al. 1993). The FLIERS are not to be confused with slow-moving blobs seen in the second ring.

In this paper, we confine our attention to the bright inner ring, where the source of excitation is clearly the UV radiation of the central star, whose effective temperature is in the neighborhood of 100,000–120,000 K. Bowen & Wyse (1939) studied the spectrum of NGC 7662 in detail; they were primarily interested in identifications and made rough estimates of line intensities. Later studies were carried out by photographic spectrophotometry and high-dispersion coudé spectra and by photoelectric spectrophotometry and with the image-tube scanner (ITS), although with spectra of reduced purity. The advent of charge coupled devices (CCDs) and the echelle spectrograph has made it possible to take advantage of high spectral resolution and accuracy. The high excitation of NGC 7662 (excitation class 9; Aller & Liller 1968), which accounts for the rich variety of lines in its spectrum, and its fairly regular structure offer the possibility of obtaining improved plasma diagnostics and abundances.

Our concern here is primarily with the optical region spectrum from 3661 to 10500 Å, as observed with the Hamilton echelle spectrograph, but observations of the near-UV region have also been secured by Likkel & Aller (1986) with an image-tube scanner. We list the ions observed and obtain the diagnostic diagram from which we can compute the ionic concentrations. Adopting a best determination of distance to the nebula, we construct a model that can represent most observed line intensities and determine the abundances based on the model and ionization correction methods—primarily with the aid of the theoretical model, we can estimate the elemental abundances similar to the empirical methods (Barker 1986 and references therein cited, and also Aller 1984) for a few elements. A final section is devoted to trace elements, essentially represented by very faint lines and represented by one or two ionization stages. For Northern Hemisphere observers, NGC 7662 is the brightest, most favorably situated high-excitation planetary nebula. Its structure is symmetrical, making it amenable to theoretical interpretation (see, e.g., Harrington et al. 1982, hereafter HSAL), wherein the line intensities are predicted with a photoionization model that takes all important physical processes into account. Thus, NGC 7662 serves as sort of keystone or prototype for studies of high-excitation PNs.

2. THE OPTICAL AND NEAR-UV OBSERVATIONS

For the near-UV region (from the limit of the Balmer series down to the atmospheric cutoff near 3000 Å), we rely primarily on the observations of Bowen and his associates with the Mt. Wilson coudé, which was recalibrated with the aid of measurements made with the Wampler-Robinson image-tube scanner at Lick Observatory (Aller & Czyzak 1979). Later, a much improved "green" tube with high sensitivity in the near-UV became available and was used by Likkel & Aller (1986) for an investigation of the O III lines of the Bowen fluorescent mechanism. In this region fall lines of He I, He II, O II, O IV, [Ne III] (auroral type), [Ne V], and [Na IV]. Note that the entrance slot has a length of 4″ and a width of 2″. The spectral purity is therefore inferior to that of the coudé or Hamilton. We attempted to guide on the bright ring in P.A. 130° (measured toward the east) in the region of highest excitation. (See Fig. 7-11 of Aller 1956.) A notch in the isophotic contours of [Ne II] 3868 and of [O III] 5007 corresponds to a region of enhanced intensity in He II 4686 and [Ne V] 3426. The He II and [Ne V] surface brightnesses in this small region of the bright ring rise by a factor of as much as 1.5; simultaneously, the [O III] and [Ne III] intensities fall 10%–25%. As the image rotates on the slit, small guiding errors can occur.

The first column of Table 1 gives the measured wavelength determined by Bowen; the second column gives the necessary digits of the laboratory identification, listed in column (3). Column (4) gives the derived intensity corrected for interstellar extinction, and the last column gives the intensities from data secured by Likkel & Aller (1986) from green-tube ITS observations. These measurements are to be preferred over the earlier data; some of the weaker, particularly O IV, lines were measured only photographically. The Bowen lines are included for completeness; they have been reviewed by Likkel & Aller.

The Hamilton echelle observations were secured with a slit width of 640 μm ($\sim 1\farcs2$) and a slit length of 4″. Since the image rotates on the slit in the course of an exposure, it is necessary to guide carefully on a selected point in the bright ring. Since the echelle pattern is larger than the 800 × 800 TI CCD chip that was most satisfactory for our purposes, we required several chip settings (see Table 2). A prism is placed in the optical train to separate out the orders; hence, these orders fall closer and closer together as the wavelength is increased. Furthermore, the pattern "fans out" toward the red, and although one chip setting (here denoted as 121) suffices for nearly all the lines shortward of 4300 Å, two chip settings (122 and 123) were employed for the region 4200–6000 Å, and three chip settings (124, 125, and 126) were used for observations longward of 6000 Å. A seventh setting (127: 4400–6900 Å) was used to record simultaneously Hα, [O III], and Hβ in one exposure. Because of changes in guiding and possible atmospheric transparency, the intensity zero point for each chip setting differed slightly, but there were sufficient numbers of lines common in adjacent chip settings to enable us to combine

TABLE 1
THE NEAR-ULTRAVIOLET REVISITED

λ_{obs} (1)	λ_{lab} (2)	Ion (3)	I(CA97) (4)	I(LA86) (5)
3121.69......	−21.7	O II	2.15	4.46
3132.91......	−32.9	O II	90.0	77.2
3187.74......	−87.7	He I	1.44	1.05
3203.23......	−03.1	He II	33	21.6
3241.72......	−41.7	[Na IV]	0.52	0.71
3265.47......	−65.5	O II	...	0.028
3299.42......	−99.4	O II	4.67	3.40
3312.35......	−12.3	O II	9.35	9.50
3340.85......	−40.7	O II	13.0	14.4
3342.68......	−42.5	[Ne III]	0.31	...
3345.89......	−45.8	[Ne V]	4.17	2.85
3362.21......	−62.2	[Na IV]	0.21	0.30
3381.25......	−81.3	O IV	0.16	...
3385.53......	−85.6	O IV	0.15	...
	−96.8	O IV	0.09	...
3403.52......	−03.6	O IV	0.16	...
3405.81......	−05.7	[O III]	0.31	0.68
	−07.4	O II	0.11	...
3411.84......	−11.8	O IV	0.24	0.77
3415.19......	−15.3	O II	0.40	...
3425.94......	−25.9	[Ne V]	10.6	9.8
3428.69......	−28.7	O II	4.25	5.68
3430.51......	−30.6	O II	0.53	...
3444.09......	−44.1	O II	18.0	32.56
3447.6	...	He I	0.06	...
3412.5	...	He I	0.07	0.14
3530.5	...	He I	0.09	0.15
3554.4	...	He I	0.14	0.154
3587.3	...	He I	0.31	0.34
3613.6	...	He I	0.16	0.31
3634.3	...	He I	0.23	0.45

TABLE 2
OBSERVATIONS FOR NGC 7662

Date (UT)	Setup	Exposure (minutes)
1988 Aug 28[a]	121	60
	122	25
	123	12.5
	124	25
	125	12.5
	126	25
1986 Nov 25[b]	122	5
	122	75
	123	90
	124	90
	125	90
	126	45
1987 Aug 3[c]	121*	5
	121*	90
	125	108.5
1987 Aug 4	121*	165
1988 Sep 30........	125	1
	125	10
	123	1
	123	10
	123	90
	122	1
	122	10
	122	90
1988 Oct 1	127*	10
	127*	90
	123	90
1989 Aug 24[d]	123	30
	122*	6
	122*	40
1990 Aug 5[e]	125	2–15

NOTE.—All observations were made with the 800 × 800 CCD chip. Setting 127 was designed so that Hα, [O III], and Hβ could be obtained with one chip setting. The echelle pattern "fans out" at longer wavelengths.* See text. For a particular exposure, a slight adjustment in horizontal position of chip was made to register a line that was otherwise missed.

[a] All exposures are in the bright ring (BR).

[b] BR, seeing, and transparency variable.

[c] BR, northeast of the star.

[d] Set on the bright blob in the outer ring.

[e] Set on various positions in the bright ring, as follows: north (major axis), 4 minutes; east (minor axis), 4 minutes; southwest, 2 and 7.5 minutes; northeast, 2 and 15 minutes, using chip setting 127 to get Hα, Hβ, and [O III] line profiles.

TABLE 3

OPTICAL REGION LINE INTENSITIES IN NGC 7662

λ_{obs}	λ_{lab}	Element	Multiplet	k_λ	I(Ham)	F(Ham)	rms (%)
3661.41......	3661.22	H I	H31	0.274	0.140	0.13	...
3662.43......	3662.26	H I	H30	0.274	0.147	0.14	...
3663.46......	3663.41	H I	H29	0.274	0.362	0.34	...
3664.67......	3664.68	H I	H28	0.274	0.328	0.31	...
3666.08......	3666.10	H I	H27	0.273	0.272	0.26	...
3667.66......	3667.88	H I	H26	0.273	0.419	0.39	...
3669.50......	3669.47	H I	H25	0.272	0.464	0.44	...
3671.40......	3671.48	H I	H24	0.272	0.817	0.77	...
3673.73......	3673.76	H I	H23	0.271	0.601	0.56	...
3676.35......	3676.36	H I	H22	0.271	0.501	0.47	...
3679.36......	3679.35	H I	H21	0.270	0.783	0.74	...
3682.83......	3682.81	H I	H20	0.269	0.776	0.73	...
3686.88......	3686.83	H I	H19	0.268	1.027	0.97	...
3691.57......	3691.56	H I	H18	0.267	0.983	0.92	...
3697.13......	3697.15	H I	H17	0.265	1.320	1.24	...
3702.38......	3702.30	He II + O III	...	0.264	0.363	0.34	...
3703.78......	3703.86	H I	H16	0.272	1.371	1.29	20.7
3705.12......	3705.02	He I	(25)	0.271	0.387	0.36	...
3707.20......	3707.24	O III	(14)	0.271	0.283	0.27	...
3710.12......	3710.40	He II + Ne II	...	0.270	0.261	0.24	...
3711.91......	3711.97	H I	H15	0.269	1.667	1.57	13.2
3715.00......	3715.08	O III?	(14)	0.269	0.418	0.39	...
	3715.60	He II	...	...	...	...	...
3721.74......	3721.94	H I	H14	0.267	2.161	2.03	16.1
	3721.83	[S III]	(2F)	...	...	...	...
3725.94......	3726.03	[O II]	(1F)	0.266	4.640	4.37	25.1
3728.69......	3728.82	[O II]	(1F)	0.265	2.418	2.28	17.7
3734.25......	3734.37	H I	H13	0.263	2.067	1.95	0.9
3736.83......	3736.76	O IV	...	0.263	0.230	0.22	...
3740.35......	3740.22	He II	...	0.262	0.149	0.14	...
	3739.92	O II	(31)	...	...	...	...
3748.54......	3748.12	He II	...	0.259	0.104	0.10	...
3750.04......	3750.15	H I	H12	0.259	2.735	2.58	2.0
3754.58......	3754.67	O III	(2)	0.258	1.119	1.05	7.1
	3757.60	N III	(11)	...	...	...	...
3757.17......	3757.21	O III	(2)	0.257	0.349	0.33	18.8
3759.73......	3759.81	O III	(2)	0.256	4.005	3.78	10.8
3768.92......	3769.07	He II	...	0.254	0.262	0.25	39.9
	3768.81	He I	(65)	...	...	...	...
3770.51......	3770.63	H I	H11	0.254	3.136	2.96	0.5
3773.85......	3774.00	O III	...	0.253	0.289	0.27	4.3
3781.57......	3781.68	He II	...	0.251	0.244	0.23	3.4
3783.97......	3783.56	[Fe V]?	...	0.250	0.121	0.11	...
3785.42......	3784.90	He I	...	0.250	0.141	0.13	...
	3785.01	O II	(95)	...	...	...	...
3791.19......	3791.26	O III	(2)	0.248	0.441	0.42	5.8
3796.23......	3796.33	He II	...	0.247	0.316	0.30	44.8
3797.81......	3797.90	H I	H10	0.246	4.599	4.35	14.4
3813.56......	3813.56	He II	...	0.242	0.373	0.35	13.1
3819.57......	3819.61	He I	(22)	0.241	0.594	0.56	17.4
3829.90......	3829.79	Ne II?	...	0.238	0.126	0.12	...
3833.65......	3833.80	He II	...	0.237	0.424	0.40	13.2
	3833.57	He I	(62)	...	...	...	...
3835.22......	3835.39	H I	H9	0.237	6.407	6.07	7.1
3857.94......	3858.07	He II	...	0.231	0.235	0.22	12.8
3868.61......	3868.71	[Ne III]	(1F)	0.228	87.06	82.60	8.2
3887.29......	3887.45	He II	...	0.223	0.385	0.37	31.5
	3889.05	H I	H8	...	...	...	...
3888.76......	3888.65	He I	(2)	0.223	15.64	14.86	3.6
3923.36......	3923.45	He II	...	0.214	0.507	0.48	25.1
3964.61......	3964.73	He I	(5)	0.204	0.370	0.35	38.8
3967.13......	3967.41	[Ne III]	(1F)	0.204	27.25	26.00	6.0
3968.29......	3968.43	He I	...	0.203	0.398	0.38	36.2
3969.90......	3970.07	H I	Hϵ	0.203	15.79	15.07	6.4
3997.29......	3997.37	[F IV]	...	0.196	0.094	0.09	...
4025.89......	4026.36	He I	(18)	0.190	1.656	1.58	10.9
4060.04......	4060.22	[F IV]	...	0.182	0.158	0.15	3.0
4067.92......	...	Line?	...	0.180	0.221	0.21	13.4
4068.70......	4068.60	[S II]	(1F)	0.180	0.434	0.42	15.8
4070.01......	4069.90	O II	(10)	0.179	0.475	0.46	17.9
4072.02......	4072.16	O II	(10)	0.179	0.158	0.15	12.0
4075.86......	4076.35	[S II]	(1F)	0.178	0.241	0.23	37.9

TABLE 3—*Continued*

λ_{obs}	λ_{lab}	Element	Multiplet	k_λ	*I*(Ham)	*F*(Ham)	rms (%)
	4097.31	N III	(1)	...	...	...	...
4097.20......	4097.27	O II	(20; 48)	0.173	1.804	1.73	4.6
4099.91......	4100.04	He II	(4–12)	0.172	0.971	0.93	32.2
4101.56......	4101.76	H I	Hδ	0.172	25.72	24.72	7.3
4103.26......	4103.37	N III	(1)	0.172	0.855	0.82	9.7
4120.69......	4120.81	He I	(16)	0.168	0.198	0.19	51.3
4128.76......	4128.80	[Fe III], C III	...	0.166	0.157	0.15	...
	4143.77	O II	(106)	...	...	...	...
4143.56......	4143.76	He I	(53)	0.163	0.173	0.17	2.6
4156.24......	4156.45	O II	...	0.160	0.095	0.09	...
	4156.49	C III	...	...	...	...	...
4163.14......	4163.30	[K V]	(1F)	0.158	0.122	0.12	36.4
4186.76......	4186.90	C III	(18)	0.154	0.304	0.29	21.6
4189.54......	4189.79	O II	(36)	0.154	0.133	0.13	61.9
4199.69......	4199.83	He II	(4−11)	0.152	1.077	1.04	39.1
4227.23......	4227.19	[Fe V]	(2F)	0.147	0.147	0.14	11.4
4251.43......	...	Line?	...	0.143	0.048	0.05	...
4267.20......	4267.18	C II	(6)	0.141	0.518	0.50	6.6
4275.53......	4275.52	O II	(67)	0.139	0.070	0.07	...
4332.28......	4332.76	O II	(65)	0.130	0.052	0.05	...
4338.83......	4338.67	He II	(4−10)	0.129	1.574	1.53	9.6
4340.50......	4340.47	H I	Hγ	0.129	45.59	44.26	4.2
4363.24......	4363.21	[O III]	(2F)	0.124	15.68	15.24	3.7
4366.87......	4366.90	O II	(2)	0.123	0.078	0.08	9.4
4376.59......	...	Line?	...	0.120	0.063	0.06	23.0
4379.41......	4379.11	N III	...	0.119	0.188	0.18	11.4
4387.90......	4387.93	He I	(51)	0.117	0.293	0.29	9.7
4414.95......	4414.91	O II	(5)	0.110	0.064	0.06	19.6
4434.71......	...	Line?	...	0.104	0.082	0.08	54.1
4437.32......	4437.55	He I	(50)	0.104	0.088	0.09	...
4448.52......	4448.21	O II	...	0.101	0.034	0.03	...
4452.80......	4452.38	O II	(5)	0.100	0.086	0.08	5.8
4458.46......	4457.95	[Fe II]?	(3)	0.098	0.107	0.10	9.4
4471.56......	4471.50	He I	(14)	0.095	1.708	1.67	5.1
4491.27......	4491.25	O II	(86)	0.090	0.039	0.04	...
4511.02......	4510.93	[K IV]	...	0.085	0.094	0.09	5.7
4517.74......	4518.18	N III	(3)	0.083	0.082	0.08	...
4523.69......	4523.60	N III	(3)	0.082	0.087	0.09	...
4534.57......	4534.57	N III	(3)	0.079	0.069	0.07	17.4
4541.70......	4541.59	He II	...	0.077	2.141	2.10	10.8
4569.02......	4568.50	O III?	...	0.070	0.024	0.02	...
4570.90......	4571.00	Mg I	(1)	0.070	0.121	0.12	42.5%
4591.39......	4590.97	O II	(15)	0.065	0.054	0.05	...
4609.57......	4609.42	O II	(93)	0.060	0.091	0.09	...
4632.24......	4631.89	O IV?	...	0.055	0.106	0.10	21.1
4634.04......	4634.16	N III	(2)	0.054	1.229	1.21	7.0
4638.63......	4638.85	O II	(1)	0.053	0.123	0.12	20.8
4640.37......	4640.64	N III	(2)	0.053	2.287	2.26	5.4
	4641.73	O II	(1)	...	...	...	...
4641.74......	4641.90	N III	(2)	0.053	0.379	0.37	9.1
4647.45......	4647.40	C III	(1)	0.051	0.589	0.58	10.2
4649.03......	4649.14	O II	(1)	0.051	0.161	0.16	13.4
	4650.84	O II	(1)	...	...	...	...
4650.32......	4650.16	C III	(1)	0.050	0.231	0.23	4.7
4651.75......	4651.35	C III	(1)	0.050	0.063	0.06	7.4
4657.78......	4658.10	[Fe III]	(3F)	0.049	0.113	0.11	15.4
4658.60......	4658.64	C IV	(3F)	0.048	0.278	0.27	12.7
4661.59......	4661.64	O II	(1)	0.048	0.105	0.10	59.2
4673.41......	4673.75	O II	(1)	0.045	0.055	0.05	...
4676.18......	4676.23	O II	(1)	0.044	0.083	0.08	13.6
4678.77......	4678.14	N II + ?	...	0.044	0.019	0.02	...
4685.61......	4685.68	He II	(3–4)	0.042	66.25	65.61	7.5
4711.26......	4711.34	[Ar IV]	(1F)	0.036	6.392	6.34	6.1
4712.92......	4713.14	He I	(12)	0.036	0.365	0.36	8.2
4714.22......	4714.25	[Ne IV]	...	0.035	0.441	0.44	16.1
4715.58......	4715.61	[Ne IV]	...	0.035	0.207	0.21	24.4
4724.16......	4724.15	[Ne IV]	...	0.033	0.525	0.52	10.3
4725.54......	4725.62	[Ne IV]	...	0.033	0.462	0.46	11.6
4740.13......	4740.20	[Ar IV]	(1F)	0.029	6.265	6.22	6.0
4859.21......	4859.32	He II	(4–8)	0.000	3.266	3.27	6.8
4861.15......	4861.33	H I	Hβ	0.000	100.00	100.00	4.5
4921.75......	4921.93	He I	(48)	−0.014	0.550	0.55	9.0
4931.43......	4931.30	[O III]	(1F)	−0.017	0.106	0.11	21.0

TABLE 3—*Continued*

λ_{obs}	λ_{lab}	Element	Multiplet	k_λ	I(Ham)	F(Ham)	rms (%)
4948.45......	4948.54	[Fe III]?	...	−0.021	0.190	0.19	27.4
	4958.90	[Fe III]	(2F)	...	...	...	...
4958.71......	4958.92	[O III]	(1F)	−0.023	368.71	370.68	10.3
4969.51......	4969.36	[b]	...	−0.026	0.127	0.13	21.5
4972.75......	4972.47	[Fe VI]	...	−0.026	0.076	0.08	...
4996.17......	...	[b]	...	−0.032	0.425	0.43	19.5
5006.73......	5006.84	[O III]	(1F)	−0.034	1223.5	1233.1	8.1
5015.77......	5015.68	He I	(4)	−0.036	0.596	0.60	16.4
5017.60......	...	[b]	...	−0.036	0.404	0.41	19.2
5048.22......	5047.74	He I	(47)	−0.043	0.194	0.20	49.0
5131.19......	5131.41	C III	5g–7h	−0.060	0.164	0.17	6.6
5146.07......	5146.06	[Fe VI]I?	(2F, 28)	−0.063	0.046	0.05	21.7
5151.02......	5151.00	[Fe III]	...	−0.064	0.023	0.02	...
5176.43......	5176.40	[Fe VI]	(2F)	−0.070	0.068	0.07	36.4
5191.81......	5191.80	[Ar III]	(3F)	−0.073	0.097	0.10	11.0
5259.09......	...	[b]	...	−0.086	0.029	0.03	...
5309.41......	5309.20	[Ca V] + ?	...	−0.097	0.058	0.06	11.8
5323.29......	5323.30	[Cl IV]	(3F)	−0.100	0.117	0.12	27.9
5335.51......	5335.18	[Fe VI]	(1F)	−0.102	0.046	0.05	37.6
5342.36......	5342.4	C II	...	−0.104	0.036	0.04	24.3
5346.23......	5346.60	He II, [Kr IV]	...	−0.105	0.122	0.13	9.8
5411.40......	5411.52	He II	(2)4–7	−0.118	4.734	4.86	8.1
5424.37......	5424.22	[Fe VI]	(1F)	−0.121	0.035	0.04	3.9
5461.31......	...	Line?	...	−0.128	0.162	0.17	19.6
5471.16......	5470.90	C IV	(7–9)	−0.130	0.054	0.06	26.8
5485.20......	5484.84	[Fe VI]	(1F)	−0.133	0.036	0.04	16.9
5517.58......	5517.71	[Cl III]	(1F)	−0.139	0.270	0.28	9.7
5537.71......	5537.88	[Cl III]	(1F)	−0.143	0.335	0.35	7.7
5577.84......	5577.34	[O I]	(3F)	−0.152	0.780	0.81	88.3
5592.42......	5592.37	O III	(5)	−0.155	0.117	0.12	9.4
5631.28......	5631.07	[Fe VI]	...	−0.164	0.022	0.02	...
5660.39......	5660.20	[b]	...	−0.170	0.017	0.02	...
5666.72......	5666.64	N II	(3)	−0.172	0.017	0.02	...
5677.39......	5676.95	[Fe VI]	(1F)	−0.174	0.018	0.02	20.3
5679.53......	5679.56	N II	(3)	−0.174	0.043	0.05	...
5720.91......	5721.10	[Fe VI]	...	−0.183	0.036	0.04	...
5754.74......	5754.64	[N II]	(3F)	−0.191	0.079	0.08	7.5
5770.10......	...	Line?	...	−0.194	0.110	0.11	...
5776.57......	5776.40	[Mn VI]?	...	−0.195	0.031	0.03	...
5780.92......	...	[b]	...	−0.196	0.027	0.03	15.3
5784.85......	5784.94	He II, [b]	(5−40)	−0.197	0.020	0.02	47.1
5789.76......	5789.72	He II	(5−39)	−0.198	0.030	0.03	19.0
5791.85......	5790.8?	He II?	...	−0.199	0.020	0.02	...
5794.99......	5794.88	He II	(5−38)	−0.199	0.022	0.02	34.5
5801.33......	5801.51	C IV	(1)	−0.201	0.308	0.32	8.5
5806.57......	5806.56	He II	(5–36)	−0.202	0.052	0.05	27.3
5812.03......	5812.14	C IV	(1)	−0.203	0.205	0.21	10.6
5814.18......	...	Line?	...	−0.203	0.044	0.05	...
5815.88......	...	[b]	...	−0.204	0.050	0.05	23.4
5820.67......	5820.43	He II	(5–34)	−0.205	0.060	0.06	11.4
5828.54......	5828.36	He II	Pf33	−0.206	0.039	0.04	13.4
5837.42......	5837.06	He II	Pf32	−0.208	0.046	0.05	9.0
5846.84......	5846.65	He II, [Kr IV]	Pf31(2F)	−0.210	0.050	0.05	9.2
5857.39......	5857.26	He II	Pf30	−0.212	0.050	0.05	14.7
5861.55......	5863.0?	[Mn V]?	...	−0.213	0.034	0.04	...
5867.97......	5867.82	[Kr IV]	...	−0.214	0.177	0.19	4.4
5869.30......	5869.02	He II	Pf29	−0.215	0.144	0.15	42.1
5875.28......	5875.67	He I	(11)	−0.216	5.513	5.79	7.4
5882.57......	5882.12	He II	Pf28	−0.217	0.074	0.08	21.3
5885.81......	...	[b]	...	−0.218	0.044	0.05	43.9
5897.57......	5896.78	He II	Pf27	−0.220	0.051	0.05	...
5913.33......	5913.24	He II	Pf26	−0.223	0.084	0.09	18.9
5932.06......	5931.83	He II	Pf25	−0.226	0.097	0.10	10.6
5944.76......	...	[b]	...	−0.228	0.060	0.06	...
5953.09......	5952.93	He II	Pf24	−0.229	0.088	0.09	6.0
5977.16......	5977.02	He II	Pf23	−0.234	0.103	0.11	7.9
6004.70......	6004.72	He II	Pf22	−0.238	0.128	0.14	7.1
6024.19......	...	[b]	...	−0.241	0.050	0.05	...
6037.12......	6036.78	He II	Pf21	−0.243	0.134	0.14	11.9
6074.14......	6074.19	He II	Pf20	−0.249	0.138	0.15	6.7
6086.56......	6086.90	[Ca V, Fe VII]	...	−0.251	0.038	0.04	...
6101.89......	6101.80	[K IV]	(1F)	−0.254	0.416	0.44	6.5
6118.51......	6118.26	He II	Pf19	−0.257	0.163	0.17	8.6

TABLE 3—*Continued*

λ_{obs}	λ_{lab}	Element	Multiplet	k_λ	*I*(Ham)	*F*(Ham)	rms (%)
6151.24......	...	[b]	...	−0.262	0.020	0.02	...
6167.01......	6166.2?	[Mn v]?	...	−0.264	0.049	0.05	...
6170.88......	6170.69	He II	Pf18	−0.265	0.177	0.19	6.6
6233.94......	6233.82	He II	Pf17	−0.275	0.191	0.20	7.8
6299.52......	...	[O I] atm.	...	−0.285	0.042	0.04	...
6300.81......	6300.30	[O I]	(1F)	−0.285	0.083	0.09	7.0
6310.74......	6310.60	He II	Pf16	−0.286	0.200	0.21	14.7
6311.95......	6312.10	[S III]	(3F)	−0.287	0.909	0.97	12.9
6363.99......	6363.78	[O I]	(1F)	−0.294	0.114	0.12	5.4
6406.45......	6406.38	He II	Pf15	−0.301	0.277	0.30	16.7
6435.09......	6435.11	[Ar v]	(1F)	−0.305	0.775	0.83	16.6
6461.91......	6461.95	C II	4f–6g	−0.309	0.072	0.08	20.6
6527.31......	6527.23	He II	...	−0.318	0.382	0.41	8.6
6548.14......	6548.03	[N II]	(1F)	−0.321	0.532	0.57	13.4
6559.98......	6560.10	He II	(4–6)	−0.322	8.969	9.66	9.5
6562.55......	6562.82	H I	Hα	−0.323	292.2	314.8	3.9
6578.48......	6578.03	C II	(2)	−0.325	0.147	0.16	25.3
6583.53......	6583.41	[N II]	(1F)	−0.326	2.016	2.17	13.5
6599.87......	6598.76	[Fe VII]?	...	−0.328	0.049	0.05	...
6678.55......	6678.15	He I	(46)	−0.338	1.453	1.57	12.1
6683.44......	6683.44	He II	Pf13	−0.339	0.481	0.52	8.9
6716.89......	6716.47	[S II]	(2F)	−0.343	0.286	0.31	16.1
6731.19......	6730.85	[S II]	(2F)	−0.345	0.459	0.50	15.0
6780.72......	6780.14	C II	(14)	−0.351	0.035	0.04	...
6891.39......	6890.88	He II	Pf12	−0.364	0.564	0.61	3.3
7005.93......	7005.90	[Ar v]	(1F)	−0.376	1.601	1.75	22.8
7063.21......	7062.40	C IV	(7–9)	−0.383	0.059	0.06	...
7065.63......	7065.28	He I	(10)	−0.383	1.878	2.05	14.3
7136.11......	7135.78	[Ar III]	(1F)	−0.391	5.584	6.11	10.5
7170.88......	7170.62	[Ar IV]	...	−0.394	0.335	0.37	12.7
7177.73......	7177.52	He II	Pf11	−0.395	0.606	0.66	6.7
7237.72......	7237.54	[Ar IV]	(2F)	−0.401	0.379	0.42	7.8
7263.36......	7262.96	[Ar IV]	(2F)	−0.404	0.282	0.31	10.3
7281.80......	7281.35	He I	(45)	−0.406	0.271	0.30	28.2
7320.36......	7319.4+	[O II]	(2F)	−0.410	0.377	0.41	6.3
7330.61......	7330.1+	[O II]	(2F)	−0.411	0.410	0.45	13.4
7530.82......	7530.83	[Cl IV]	(1F)	−0.431	0.415	0.46	11.7
7593.00......	7592.75	He II	Pf10	−0.436	1.113	1.23	5.3
7713.11......	7713.11	O IV	(21)	−0.448	0.138	0.15	34.2
7726.56......	7726.2	C IV	(81)	−0.449	0.202	0.22	10.4
7751.78......	7751.43	[Ar III]	(1F)	−0.451	1.757	1.95	8.0
8046.00......	8046.27	[Cl IV]	(1F)	−0.477	0.880	0.98	11.3
8197.06......	8196.48	C III	(43)	−0.489	0.339	0.38	6.7
8237.40......	8236.78	He II	Pf9	−0.492	1.591	1.78	2.2
8277.63......	8276.31	H I[a]	P32	−0.496	0.099	0.11	...
8282.43......	8281.12	H I[a]	P31	−0.496	0.127	0.14	...
8287.55......	8286.43	H I	P30	−0.496	0.109	0.12	...
8293.07......	8292.31	H I	P29	−0.497	0.179	0.20	...
8296.94......	8298.84	H I atm.?	P28	−0.497	0.146	0.16	...
8301.34......	...	Line?	...	−0.497	0.024	0.03	...
8307.99......	8306.12	H I[a]	P27	−0.498	0.029	0.03	...
8313.48......	8314.26	H I	P26	−0.498	0.099	0.11	...
8314.89......	8315.1	C III	5g–6h	−0.499	0.028	0.03	...
8319.95......	8319.9	He II	...	−0.499	0.023	0.03	...
8324.50......	8323.43	H I	P25	−0.499	0.103	0.12	21.0
8334.32......	8333.78	H I	P24	−0.500	0.132	0.15	17.3
8345.75......	8345.55	H I	P23	−0.502	0.209	0.23	53.2
8359.61......	8359.66	H I, He II	P22+?	−0.504	0.144	0.16	20.6
8375.24......	8374.48	H I	P21	−0.507	0.149	0.17	11.1
8393.28......	8392.40	H I	P20	−0.509	0.214	0.24	...
8413.85......	8413.32	H I	P19	−0.512	0.205	0.23	28.1
8438.64......	8437.96	H I	P18	−0.516	0.265	0.30	3.8
8467.51......	8467.26	H I	P17	−0.521	0.326	0.37	13.1
8479.63......	8480.73	[Cl III]	(3F)	−0.523	0.057	0.06	...
8502.98......	8502.49	H I	P16	−0.526	0.347	0.39	7.2
8545.93......	8545.38	H I	P15	−0.532	0.415	0.47	2.1
8598.96......	8598.39	H I	P14	−0.540	0.579	0.66	4.8
8665.52......	8665.02	H I	P13	−0.550	0.711	0.81	2.6
8725.84......	8727.2	[C I]	(1)	−0.559	0.080	0.09	...
8733.22......	8733.43	He I	(6/12)	−0.560	0.083	0.10	...
8749.34......	8750.48	H I	P12	−0.562	0.891	1.01	11.8
8860.88......	8759.1	He II	(6–24)	−0.578	0.155	0.18	...
8863.36......	8862.79	H I	P11	−0.578	1.154	1.32	2.8

TABLE 3—*Continued*

λ_{obs}	λ_{lab}	Element	Multiplet	k_λ	I(Ham)	F(Ham)	rms (%)
9015.53	9014.91	H I	P10	−0.599	1.589	1.82	9.2
9069.28	9068.90	[S III]	(1F)	−0.606	5.425	6.24	8.0
9212.56	9213.24	He I	(7/9)	−0.612	0.036	0.04	...
9229.11	9229.02	H I	P9	−0.612	2.227	2.56	44.6
9531.16	9531.00	[S III]	(1F)	−0.620	23.50	27.10	22.4
9546.18	9545.97	H I[a]	P8	−0.620	1.538	1.77	9.9
9762.20	9762.1	He I	(6−15)	−0.625	0.129	0.15	...
10049.53......	10049.38	H I	P7	−0.632	4.082	4.72	3.1
10123.62......	10123.61	He II	(4–5)	−0.633	14.99	17.34	...

NOTE.—Identification of He I from Osterbrock et al. 1992. ?: Unlikely or doubtful identification. See Baluteau et al. 1995 and Péquignot & Baluteau 1988 for the identification and transition notation of the far-red He I lines in cols. (3) and (4).

[a] Lines affected by the atmosphere.

[b] These unidentified lines are seen in other PNs, i.e., IC 4997, NGC 7027, and NGC 7009.

intensities. For each chip setting, one must obtain an observation of the Th-Ar arc, a lamp to set wavelengths, and a dome-quartz lamp to fix a flat field, i.e., to allow for sensitivity fluctuations from chip to chip, and a comparison star of known energy distribution. The reduction procedures are described by Hyung (1994).

The optical line intensity data are summarized in Table 3. Successive columns give the measured wavelength, the wavelength of the most probable identification, and the element and multiplet number from Moore's tabulation (1974, 1993) and also from the work of T. Feklistova & A. F. Kholtygin (A New Atomic Line Catalogue for Planetary Nebulae, private communication, 1996). The sixth column gives the intensity corrected for interstellar extinction on the scale $I(4861) = 100.0$ with an extinction parameter of $C = 0.10$ [$C = \log I(\mathrm{H}\beta)/F(\mathrm{H}\beta)$ using Balmer line ratios such as $F(\mathrm{H}\alpha)/F(\mathrm{H}\beta)$ and $F(\mathrm{H}\gamma)/F(\mathrm{H}\beta)$ and a comparison of Balmer and Paschen lines]; this is lower than values found by other observers, e.g., $\sim$0.2 from the Balmer decrement and a comparison of radio and Hβ measurements (Stasinska et al. 1992) or 0.23 (HSAL).

Extensive determination of the accidental errors for individual lines may be found because of the large number of line intensity measurements made with equivalent chip settings and comparable exposures. These observations were made in the early stages of our program. The errors include the effects of guiding errors from frame to frame but not the effects of errors in the response function or in atmospheric transparency. For $I < 0.5$, the average error is 23%; for $0.5 < I < 1.0$, the mean error is 17%; and for $1.0 < I < 10$, the mean error is about 8%; while for $I > 10$, the mean error is around 6%.

Lines of atoms and ions represented in the spectrum of NGC 7662 include the following: H I, He I, He II, [C I], C II, C III, C IV, N II, [N II], [N III], O I, [O I], [O II], [O III], O IV, O V, [F IV], [Ne III], [Ne IV], [Ne V], [Na IV], Mg I, Si III, [S II], [S III], [S IV], [Cl III], [Cl IV], [Ar III], [Ar IV], [Ar V], [K IV], [K V], [Ca V], [Mn V], [Fe III], [Fe V], and [Fe VI]. The lines of C III, C IV, N III, N IV, N V, O IV, Si III, and [Mg V] suited for abundance determinations all lie shortward of 3000 Å.

3. DIAGNOSTICS AND IONIC CONCENTRATIONS

Several diagnostic possibilities are offered for NGC 7662, and we can be further guided by theoretical studies, e.g., those similar to the HSAL study. Diagnostic line ratios suitable for fixing (N_ϵ, T_ϵ) are listed in Table 4. A compilation of recent electronic collision strengths is given in Hyung & Aller (1996).

Figure 1 gives the diagnostic diagram. In his region 2, which is most nearly comparable to the region we have observed, Barker (1986) finds $T_\epsilon = 13{,}100$ K. From the I(Balc)/I(4861) ratio, he finds $T_\epsilon = 15{,}400$ K, and from He II $I(1402)/I(1640)$, $T_\epsilon = 13{,}600$ K. The theoretical studies of model in § 4 indicate T_ϵ([O III]) $\sim$ 13,100 K, while T_ϵ([O II]) $\sim$ 12,100 K. The diagnostic line of [Ar III] indicates $T_\epsilon \sim 13{,}600$ K, while the model gives $T_\epsilon \sim 13{,}000$ K. From the [O III] $\lambda\lambda$[4959 + 5007]/4363 ratio and $N_\epsilon \sim 8000$ cm^{-3}, we get $T_\epsilon \sim 12{,}500$ K. For low-excitation ions it may be lower, e.g., $\sim$8500 K for [N II]. For T_ϵ([O II]) = 12,500 K, we find $N_\epsilon \sim 17{,}000$ cm^{-3}. There may be at least two N_ϵ regimes predominating in this PN: (1) a domain with $N_\epsilon \sim 3000$ cm^{-3}, as suggested by [Ar IV]; and (2) a higher density domain with $N_\epsilon \sim 17{,}000$ cm^{-2}, as suggested by the nebular and auroral lines of [O II]. Using the latest results by Keenan et al. (1996), the [S II] data suggest an even higher density and a low T_ϵ. The [S II] lines may be produced at an interface between H I and H II regions.

Rowlands et al. (1989) compared the 34.3 μm line of [Ne V] with the 3426 Å line to get $T_\epsilon = 13{,}200$ K in the hot Ne V zone, and [O IV] 26.9 μm and 1400 Å line to get $T_\epsilon = 14{,}400$ K in the O IV zone, which is in reasonable agreement with theoretical predictions. On the other hand, from a comparison of the [Ar IV] $\lambda\lambda$4711, 4740 nebular-type tran-

TABLE 4

DIAGNOSTIC LINE RATIOS

Ion	Lines	Ratio	Determines
[N II]	$I(\lambda6548^a + \lambda6583^a)/I(\lambda5755^a)$	31.49	T_ϵ
[O II]	$I(\lambda3726)/I(\lambda3729)$	1.919	N_ϵ
[O III]	$I(\lambda4959 + \lambda5007)/I(\lambda4363)$	101.5	T_ϵ
[S II]–	$I(\lambda6731^a)/I(\lambda4069^a + \lambda4076^a)$	0.680	N_ϵ, T_ϵ[b]
[S III]	$I(\lambda9069 + \lambda9531^c)/I(\lambda6312^a)$	31.82	T_ϵ
[Ar III]	$I(\lambda7136 + \lambda7751)/I(\lambda5191)$	75.68	T_ϵ
[Ar IV]	$I(\lambda4711)/I(\lambda4740)$	1.020	N_ϵ
[Cl IV]	$I(\lambda5323^a)/I(\lambda8046^a)$	0.133	T_ϵ

NOTE.—Note that inclusion of the [Ar IV] auroral type transitions enables T_ϵ and N_ϵ to be determined. The temperature thus obtained, 20,000 K, seems too high for the [Ar IV] zone.

[a] These lines are so weak, i.e., $I < 1.0$, that the diagnostics are very uncertain.

[b] A weak [S II]λ6716, which is contaminated by "drip" from strong Hα, is not used.

[c] Affected by atmospheric extinction.

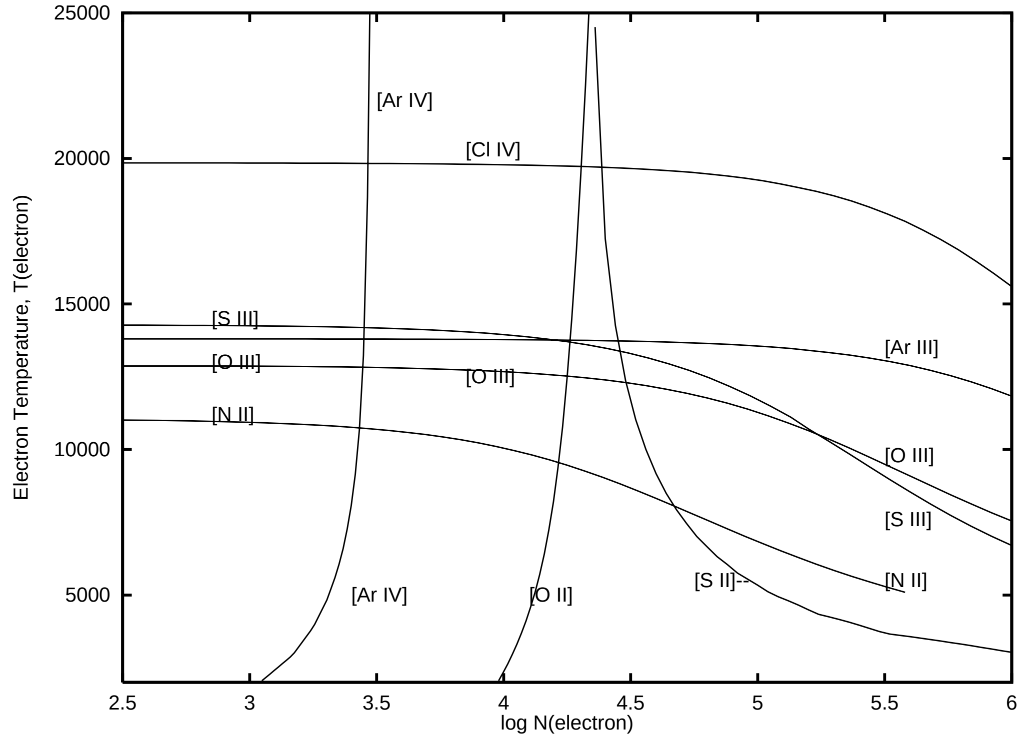

FIG. 1.—Diagnostic diagram for NGC 7662: T_ϵ vs. log N_ϵ. Here [S II]– refers to the transauroral to nebular-type transition, ($\lambda\lambda$4069 + 4076)/($\lambda\lambda$6731). See Table 4.

sitions with the $\lambda\lambda$7171, 7263 auroral-type lines, Keenan et al. (1997) solved for both the electron temperature and density: $T_\epsilon = 20{,}000$ K and log $N_\epsilon = 3.8$. The density seems reasonably well established, but the T_ϵ situation is far from satisfactory. The temperature in the [Ne V] zone cannot be less than that in the [Ar IV] zone. The [Ne V] measurements required IR and near-UV measurements made with different equipment and involving different regions of the nebula. The red [Ar IV] lines may be affected by unknown blends.

Once the proper diagnostic ratios have been established, one can choose the representative electron temperature, T_ϵ, and electron density, N_ϵ. We may now obtain the ionic concentrations by well-known formulae (see, e.g., Aller 1984; Osterbrock 1989), updated for the most recent and reliable values of atomic constants. For most ions, we take the representative electron temperature and density, but for highly ionized stages, we may be guided by a model prediction in § 4. Here, we do not introduce a refinement by making use of model predictions described in the next section for the T_ϵ fluctuations. We adopted $T_\epsilon = 12{,}500$ K and $N_\epsilon = 8000$ cm^{-3} for most ions, but for He II, we take $T_\epsilon = 13{,}500$ K. See also Table 18 of HSAL, which gives results for their model II. HSAL did not consider certain ions in the optical region, e.g., [Ne V], [Ar IV], [Ar V], and [Cl IV], that are considered in the present investigation.

The first column of Table 5 gives the ion involved, the second the wavelength, the third the adopted intensity, and the last column the value of N(ion)/N(H$^+$). For the far-UV lines of ions of carbon and nitrogen, we rely on the measurements of Barker for his region 2 in the bright ring, which most nearly matches the position that we observed. For the *IUE* [C II], [O IV], Mg II, and Si III], which are not available from Barker, we used the measurements by HSAL.

4. THEORETICAL MODEL

A description of the modeling procedures, including references to selected atomic parameters, may be found in Hyung (1994), and a later update can be found in Hyung & Aller (1996). As in our previous studies, e.g., IC 2165 (Hyung 1994), we construct a shell model with a central star energy distribution from Hubeny's (1988) non-LTE model atmospheres.

The choice of model atmosphere for the central star fixes the level of excitation of the spectrum. To find the proper central stellar atmospheric flux, we carried out an initial model calculation with Hubeny's (1988) non-LTE atmospheres corresponding to HSAL model II temperatures $T_* \sim 120{,}000$ K. This stellar temperature proved unsatisfactory, as it failed to predict [O II]/[O III], and the predicted electron temperatures were relatively too high for adopted input abundances. In these trials, we assumed a distance of 800 pc (determined by a kinematics method; Hajian & Terzian 1996, hereafter HTz). We adopted a constant H density for the shell. Choosing trial values of $N_H =$ 3000, ..., 10,000 atoms cm^{-3}, we finally settled on 6000 atoms cm^{-3} in a density-bounded configuration. After laborious trials, we found that a successful prediction of the spectrum would require a model atmosphere with $T_* =$ 105,000 K.

The details of our adopted standard model are described in Table 6. The stellar energy distribution was that of $T_{\rm eff} =$ 105,000 K and log $g = 5.7$ with He/H = 0.093 + nebular heavy element distribution in the central star. The present shell model or HSAL model II would be suitable for abundance determinations. Even better would be a "composite-shell" model, similar to the type employed for various PNs

TABLE 5

IONIC CONCENTRATIONS

Ion (1)	Wavelength (2)	I (Line) (3)	N(ion)/N(H⁺) (4)
He I	4471	1.708	0.035
	5876	5.513	0.033
	6678	1.453	0.036
He II	4686	66.25	0.058
[C II]	2325, 2329	(10.9)H	5.07(−6)
C III]	1907, 1909	(517)B	2.79(−4)
C IV]	1549, 1551	(1266)B	5.13(−4)
[N II]	6548, 6584, 5755	2.627	2.36(−7)
N III]	1747–	(11)B	2.75(−5)
N IV]	1487–	(21)B	6.72(−5)
N V	1240–	(22)	5.92(−5)
[O I]	6300, 6363, 5577	0.977	5.81(−7)
[O II]	3726, 3729, 7319, 7330	7.85	2.32(−6)
[O III]	4959, 3463, 5007	1608	2.25(−4)
[O IV]	1402–	(27.0)H	4.50(−4)
[F IV]	3997, 4060	0.252	5.72(−8)
[Ca V]	5309	0.058	2.20(−8)
Mg II	2800–	(0.8)H	1.11(−8)
Si III]	1883–	(8.0)H	9.20(−7)
[S II]	6717, 6731,4068, 4076	0.745	1.59(−8)
[S III]	6312, 9069, 9532	29.83	6.96(−7)
[S IV]	10.5 μm	124	4.02(−6)
[Na IV]	4242, 3362	1.01	6.24(−7)
[Cl III]	5517, 5537, 8481	0.662	2.67(−8)
[Cl IV]	5323, 7530, 8045	1.412	5.63(−8):
[Ar III]	7135, 7751	7.341	3.07(−7)
[Ar IV]	4711, 4740, 7240, 7263	13.653	7.39(−7)
[Ar V]	6435, 7005	2.376	1.70(−7):
[K IV]	6102	0.416	6.59(−8)
[K V]	4163	0.122	3.24(−8)
Ne III	3868, 3967	114.3	3.18(−5)
Ne IV	2423, 2425, 4715, 4725	94.64	5.51(−5):
Ne V	3346, 3426	12.65	4.55(−6)

NOTE.—Adopted $T_\epsilon = 12{,}500$ K and $N_\epsilon = 8000$ cm^{-3} (except for ions as noted in text). $I(4861) = 100$. $X(-Y)$ implies $X \times 10^{-Y}$. : = Uncertainty estimated ≥ 50%. B: *IUE* data from Barker 1986 for his position 2. H: *IUE* data from HSAL.

TABLE 6

DETAILS OF MODEL

Parameter	Value
Distance (pc)	800
Shell N_H (cm^{-3})	6000 (density bounded):
R_{in}, R_{out} (pc)	0.025, 0.035 (9″.0)
M_{dust}/M_{gas}	0.005
$F(H\beta)_{obs}$ (ergs cm^{-2} s^{-1})	1.30–1.70 × 10^{-11} [a]
$F(H\beta)_{pred}$ (ergs cm^{-2} s^{-1})	1.70 × 10^{-10}
Nebular $\langle T_\epsilon \rangle$ (K)	13,000
Central star T_* [b] (K)	105,000 (log g = 5.7)
Central star R_*	0.15 $R_\odot$ ($L_* = 2470\ L_\odot$)
Predicted magnitude:	
B	12.4
V	12.7

[a] Extinction-corrected flux assuming $C = 0.1$–0.23.

[b] Hubeny non-LTE model atmosphere with He/H = 0.093 + nebular heavy elements.

in our previous investigations, but the effort would be worthwhile only when high spatial resolution and kinematical data are at hand. Such a refinement must await the analysis of images obtained by adaptive optics supplemented by high-dispersion spectral line profiles secured at various points on the disk, which can be supplied by our available Hamilton data. With this detailed information at hand, we will be able to prepare a theoretical paper on the nebular structure with a more sophisticated composite-shell model, described in Hyung & Aller (1996).

The outer boundary of the shell is material bounded, ~9″.0, and the shell is assumed to be homogeneous. No filling factor is introduced in the shell gas. We assume a central star radius of $R_* = 0.15\ R_\odot$ and, as a result, $L_* = 2470\ L_\odot$. We assumed that in the radiating strata the dust-to-gas ratio is $M_{dust}/M_{gas} = 0.005$. Thus, for the resonance UV lines, e.g., C IV λλ1549, 1551, the dust effect has been corrected in the prediction using the method described in HSAL or Hyung (1994). The observed absolute Hβ flux is $F(H\beta) = 1.02 \times 10^{-10}$ ergs cm^{-2} s^{-1}, and the absolute intrinsic flux is $F_{corr}(H\beta) = (1.26\text{–}1.70) \times 10^{-10}$ for $C = 0.10$–0.23 (see Table 7). For a distance of 800 pc, the model reproduces the absolute Hβ flux to within observational errors. The observed visual magnitude is $m_v = 13.8$, and accordingly the intrinsic visual magnitude $m_{v0} = 12.8$ using the $E_{B-V} = 0.156$ (from $C = 0.23$) and corresponding total extinction A_v here taken as $3.1E_{B-V}$. The predicted intrinsic visual and blue magnitudes are $m_v = 12.4$ and $m_b = 12.7$, respectively.

Table 8 compares observed and predicted intensities. The Hamilton echelle data and *IUE* data are given in column (3), while column (4) lists the predicted intensities from the model. All of the values are on the scale of $I(H\beta) = 100$.

For most ions, the agreement between observed and predicted intensities is good, but in some cases, discordances

TABLE 7

SUMMARY OF BASIC DATA FOR NGC 7662, PK 106−17°1′

Parameter	Value
α(2000) (h m s)	23 25 53.8
δ(2000) (° ′ ″)	+42 32 06
l (deg)	106.5
b (deg)	17.6
Diameter (arcsec)	17 (double ring structure)
Radial velocity (km s^{-1})	−13.2 ± 0.7
Expansion velocity (km s^{-1}):	
[O II]	27.5
[N II]	29
log $F(H\beta)$ (ergs cm^{-2} s^{-1})	−9.99 (whole nebula)
Interstellar extinction, *C*	0.1–.23
$F_{corr}(H\beta)$ (ergs cm^{-2} s^{-1})	(1.26–1.70) × 10^{-10}
Distance (kpc):	
This work	0.79
HTz	0.75
CKS	1.16
VSZ	1.11
Z95	1.17
Dust (log M_{dust}/M_{gas})	−2.97 (LNP)
Central star (PNN):	
B	13.6
V	13.3
T(PNN) (K)	100,000
T(eff) (K)	122,000 (HSAL)

NOTE.—CKS: Cahn, Kaler, & Stanghellini 1992; HSAL: Harrington et al. 1982; HTz: Hajian & Terzian 1996; LNP: Lenzun, Natta, & Panagia 1989; VSZ: Van der Steene & Zijlstra 1995; Z95: Zhang 1995. Unless otherwise indicated, data are from Acker et al. 1992.

TABLE 8

COMPARISON OF OBSERVED AND PREDICTED INTENSITIES

Element/Ion (1)	λ (2)	I(obs) (3)	Model (4)
He I	5876	5.51	4.95
	6678	1.45	1.18
	4471	1.71	1.76
He II	4686	66.25	70.11
	5412	4.73	5.87
C II	2325, 2328	10.9H	10.73
	4267	0.52	0.14
C III	1907, 1909	517B	471.4
C IV	1548, 1551	1266B	1208
N II	6584	2.02	1.93
	6548	0.53	0.67
	5755	0.08	0.07
N III	1747–52	11B	14.8
N IV	1487–	21B	25.4
O II	3726	4.64	3.59
	3729	2.42	1.56
	7321, 7322	0.38	0.43
	7332, 7333	0.41	0.35
O III	4363	15.68	20.87
	4959	642.0	469.1
	5007	1223.5	1351.3
O IV	1403–1413	27.0H	21.95
Ne III	3868	87.06	88.468
	3969	15.79	26.39
Ne IV	2422, 2425	93H	95.96
	4725, 4727	0.99	0.76
Ne V	3347	2.85	5.90
	3426	9.80	16.1
Mg II	2800–	0.8H	0.75
Si III	1883, 1892	8.0H	9.7
S II	4068	0.43	0.06
	4076	0.24	0.02
	6717	0.29	0.06
	6731	0.46	0.11
S III	6312	0.91	0.57
	9069	5.43	6.68
	9531	25.5	16.4
S IV	10.5 μm	124	164.16
Cl III	5518	0.27	0.16
	5538	0.34	0.26
Cl IV	7530	0.41	0.48
	8046	0.88	1.12
Ar III	7136	5.58	1.70
	7751	1.76	0.41
Ar IV	4711	6.39	9.44
	4740	6.26	12.3
	7238	0.38	0.28
	7265	0.28	0.31
	7172	0.34	0.38

NOTE.—B: *IUE* data from Barker 1986. H: *IUE* data from HSAL.

are large, especially for [S II] and [Ar III]. The agreement for both He I and H II is good. The agreement for C is also good except for the recombination C II λ4267 line, attributed to recombination. As in a number of other PNs, the C^{++} abundance deduced from the λ4267 line exceeds that found from the collisionally excited UV λλ1907, 1909 lines. The problem has been intensively studied by Barker (1987, 1991), who suggests that λ4267 may be blended with a high-excitation line of unknown origin. Other lines of the same cascade sequence that produces λ4267 are λ7236, which is blended with [Ar IV] λ7231, which appears to be lost in telluric absorption. Two other lines of multiplet number 2 include λ6582, which is lost in [N II] λ6583, and λ6578.02, which is detected as a faint feature, with $I = 0.16$.

Predictions for the ions of N, O, Ne, and Cl seem generally successful. The predicted intensities of [O I], which seem too weak, are not listed, because the model does not include large neutral blobs. Similarly, the observed [S II] is stronger than the predicted. Possibly the [S II] radiation is emitted in neutral region strata or an interface between H I and H II domains. The prediction for [S III] agrees as well as could be expected in view of the fact the [S III] λλ9069, 9531 line is affected by water-vapor absorption.

Rare elements are mostly represented by single ionization stages, except for potassium. Potassium is represented by [K IV] and [K V]. Si is represented by a single ionization stage of Si III], sodium by [Na IV], calcium by [Ca V], magnesium by Mg II, and fluorine by [F IV]. Hence, agreement for these ions can be assured, and the abundances of these elements must be found from a single ionization stage whether we use a nebular model or the ionization correction factor (ICF) method. For example, the [Ca V] λ5309 line ($I = 0.058$) is fitted by $N(\mathrm{Ca})/N(\mathrm{H}) = 5.0 \times 10^{-8}$, etc. Thus, the seventh column of Table 9 recapitulates the model results.

5. THE ABUNDANCE PROBLEM

Since the pioneering efforts of Bowen & Wyse (1939) and Wyse (1942), many attempts have been made to determine the chemical composition of NGC 7662 using gradually improving atomic data, theoretical concepts, and observational data. Aller & Menzel (1945) used the then newly developed theoretical approach of the Harvard program; Aller (1957) employed new photographic and photoelectric data and Seaton's (1979) collisional cross sections for a new analysis. Among more recent investigations, we may mention those of Péquignot (1980), Benvenuti & Perinotto (1981), Peña & Torres-Peimbert (1981), Aller & Czyzak (1983), Harrington et al. (1982), and Barker (1986).

Two popular approaches to PN compositions have been via models and by empirical formulae often coupled with measurements made at several points in the nebular image. The most painstaking investigation of NGC 7662 by the model method is that by HSAL. There are two principal forms of the model method; you can predict individual line intensities and modify parameters until a good fit is obtained, or you strive for the best fit for lines covering a huge range of excitation and then use the model as a device for deriving ICFs. Two obvious limitations of the model method may be recalled: geometrical irregularities in the nebula and small-scale irregularities. (See Walker & Aller 1970; and Capriotti, Cromwell, & Williams 1971.)

An alternative approach that is the only one practical for manifestly inhomogeneous, often large, PNs and useful even for objects such as NGC 7662, which are good candidates for modeling, is the method employed by Barker. At several positions on the nebular image, one measures the spectrum, derives ionic concentrations, and then employs the usual recipes to get the ICFs. NGC 7662 is similar to NGC 3242 (Barker 1986). An example of a large irregular object is NGC 6853 (Barker 1984). Several studies have been carried out for the Ring Nebula (Hawley & Miller 1977; Aller 1976; Barker 1980, 1982).

The abundances of individual elements are given in Table 9. Here, the first two columns give the element involved and the sum of the ions observed. Column (3) gives the ICF derived from the model, and in columns (4), (5), (6), and (7), we list the abundances determined by the present ICF method, Barker's empirical one, the HSAL model II, and

TABLE 9

ELEMENTAL ABUNDANCES

ELEMENT (1)	$\sum N(\text{ion})/N(\text{H}^+)$ (2)	ICF (3)	N(elem)/$N(\text{H}^+)$ ICF-M (4)	Barker (5)	HSAL (6)	Model (7)	MEAN[a] (8)	SOLAR[b] (9)
He	0.093	1.000	0.093	0.093	0.094	0.093	0.11	0.098
C	7.97(−4)	1.190	9.48(−4)	6.8(−4)	6.2(−4)	4.5(−4)	6.48(−4)	3.6(−4)
[N II]	2.36(−7)	200.0	4.72(−5)	...	6.0(−5)	6.0(−5)	1.40(−4)	1.1(−4)
N sum	1.54(−4)	1.002	1.54(−4)	1.1(−4)	...	...	...	...
O	6.83(−4)	1.025	7.00(−4)	4.3(−4)	3.6(−4)	3.5(−4)	4.93(−4)	8.5(−4)
Ne	9.15(−5)	1.002	9.16(−5)	9.1(−5)	7.0(−5)	6.3(−5)	1.25(−4)	1.2(−4)
S	4.73(−6)	1.002	4.74(−6)	4.2(−6)	1.5(−6)	7.0(−6)	8.08(−6)	1.6(−5)
Ar	1.22(−6)	1.065	1.30(−6)	1.5(−6)	...	2.0(−6)	2.42(−6)	3.6(−6)
Cl	8.30(−8)	1.873	1.55(−7)	...	...	1.5(−7)	1.66(−7)	3.2(−7)
Na	6.24(−7)	1.799	1.12(−6)	...	...	1.1(−6)	1.50(−6)	2.1(−6)
Ca	2.20(−8)	2.299	5.06(−8)	...	...	5.0(−8)	1.10(−7)	1.6(−6)
Mg	1.11(−8)	83.33	9.33(−7)	...	8.0(−7)	8.0(−7)	2.70(−5)	3.6(−5)
F	5.72(−8)	1.883	1.08(−7)	...	...	1.1(−7)	...	...
K	9.83(−8)	1.202	1.18(−7)	...	...	1.3(−7)	9.00(−8)	1.3(−7)
Si	9.20(−7)	6.897	6.35(−6)	...	6.0(−6)	5.0(−6)	...	1.6(−5)

NOTE.—$X(-Y)$ implies $X \times 10^{-Y}$.

[a] See text.

[b] Solar abundances by Grevesse & Anders 1989.

the present model study, respectively. Column (8) presents the average abundances for non–type I PNs from Kingsburgh & Barlow (1994; their Table 14) for He, C, N, O, Ne, S, and Ar. For Cl, Na, Ca, and K, we take the mean abundances from Aller & Czyzak (1983). The uncertain abundance of Mg applies to NGC 6741 and is taken from Aller, Keyes, & Czyzak (1985). The solar abundances by Grevesse & Anders (1989) are given in the last column.

Helium.—The census of helium atoms is virtually complete, as we observed He I and He II. The agreement with HSAL and Barker is good.

Carbon.—Note that the abundance determinations for this element show a large spread; the ICF method gives a result that differs from the pure model method by a factor of 2. For the *IUE* C III] and C IV], we rely on Barker's observations for his position 2, which most nearly coincides with our position. Likewise for C II, which is unavailable from Barker's position 2, we have relied on HSAL's *IUE* observations.

Nitrogen.—An often-employed method is to get the abundance of nitrogen with the aid of ICFs. NGC 7662 has weak [N II] lines. The abundance of nitrogen from [N II] with the empirical ICF gives a larger value than that of the model method, i.e., 1.68×10^{-4} with Barker's ICF = 711 for his position 2. If we use Barker's observations of the UV N III] and N IV] lines and compute the sum of all the observed ions, there still emerges a larger value, 1.54×10^{-4} than HSAL's derivation. The abundance of nitrogen from [N II] with the aid of a model ICF = 200.0 turns out to be a seemingly more plausible value than the empirical estimate. We prefer the model value of 6.0×10^{-5} for N abundance.

Oxygen.—Note that HSAL, our model, and Barker are in fair agreement. Even Kingsburgh & Barlow (1994) fits pretty well. However, the sum of all the observed ions is not in agreement, partially because of relatively low T_ϵ for the [O IV]. One must use great caution in choosing T_ϵ for a determination of the ionic concentrations, especially when the empirical method is employed.

Neon.—Nearly all neon atoms radiate as [Ne III], [Ne IV], or [Ne V], and the chief uncertainty here is T_ϵ in the Ne^{+3} and Ne^{+4} zones. Obviously the uncertainty in electron temperature of the hot zone is of utmost importance. We might rely on our model to get T_ϵ. (See Rowlands et al. 1989.) We adopt the ICF result, 9.1×10^{-5}, for Ne.

Chlorine.—Chlorine seems well accounted for. With the aid of the model, we can make reasonable estimates of T_ϵ for the appropriate zones and the abundance. Probably most chlorine atoms radiate as [Cl II], [Cl III], or [Cl IV], yielding an abundance of 1.5×10^{-7}.

Argon.—We are inclined to the model result for argon, 2.0×10^{-6}. All of the important ionization stages are accounted for. The very high T_ϵ of the [Ar IV] zone found by Keenan et al. (1997) does not seem to fit the results by Rowlands et al. (1989).

Sulfur.—S^{++} and S^{++} account for only a minority of sulfur ions. We used the measurements of Beck et al. (1981) to estimate the abundance of the S^{+3} ion. The difference between HSAL and Barker's results and our own arises from the way [S IV] was handled.

Ions of rare elements.—Relatively rare elements are often represented by only single ions or a scattering of ionization stages such as those of iron. The elements of fluorine, sodium, potassium, and calcium are revealed by [F IV], [Na IV], [K IV], and [Ca V]. To estimate the abundances of these elements, we will have to rely on a model.

6. CONCLUDING REMARKS

The general, overall abundance pattern suggested by our ICF methods is similar to that found by Barker (1986), while the model study results are similar to that of HSAL. Compared with the previous studies, we, however, have more numerous line measurements in the optical wavelength region than Barker or HSAL, and further improvements may be forthcoming as improved atomic data become available. As an example, we may cite results for the important ion S^+, where the electronic collisional rates for the ground configuration may differ by a factor of up to 2 from previous results (Keenan et al. 1996).

Carbon is more abundant than in the Sun. Nitrogen is questionable; we saw that the N abundance from [N II] required a huge, uncertain ICF factor, while the inclusion of the UV data gave a larger result. If N is overabundant, it is probably so by a small factor. If we believe the result by HSAL or our model, N abundance in NGC 7662 appears to be less than that in the Sun by a factor of 2. The other elements, O, Ne, S, Cl, and Ar, are much less abundant than in the Sun, in harmony with Barker's suggestion that the precursor star was "metal" deficient.

We adopted probably a more accurate distance. The predicted visual magnitude and the overall nebular line intensities generally are in accord with those observed. Thus, with the selected PN distance from HTz, the adopted planetary nebula nucleus (PNN) temperature, and surface gravity and luminosity, we should have the PNN mass. The Schönberner (1981) track gives a mass of about 0.61 $M_{\odot}$. An age of about 8000 yr is implied.

This research was supported in part by the National Science Foundation through grants AST 90-14133, AST 93-13991, and AST 94-16985 to the University of California, Los Angeles, and by Star Research Grant through Star 96-5700-403 to the KAO/BOAO sponsored by Korea MOST. We are indebted to Dr. Lauren Likkel, who measured all the UV lines from the green-tube series. We want to express our gratitude also to Timothy Barker, who offered a number of valuable suggestions.

REFERENCES

Acker, A., Ochsenbein, F., Stenholm, B., Tylenda, R., Marcout, J., & Schohn, C. 1992, Strasbourg-ESO Catalogue of Galactic Planetary Nebulae (Garching: ESO)
Aller, L. H. 1956, Gaseous Nebulae (London: Chapman & Hall)
———. 1957, ApJ, 125, 84
———. 1976, PASP, 88, 574
———. 1984, in Physics of Thermal Gaseous Nebulae (Dordrecht: Reidel)
Aller, L. H., & Czyzak, S. J. 1979, Ap&SS, 62, 387
———. 1983, ApJS, 51, 211
Aller, L. H., Keyes, C. D., & Czyzak S. J. 1985, ApJ, 296, 492 (AKC85)
Aller, L. H., & Liller, W. 1968, in Nebulae and Interstellar Matter, ed. B. M. Middlehurst & L. H. Aller (Chicago: Univ. Chicago Press), chap. 9
Aller, L. H., & Menzel, D. H. 1945, ApJ, 102, 239
Balick, B. 1987, AJ, 94, 671
Balick, B., Rugers, M., Terzian Y., & Chengular N. 1993, ApJ, 411, 773
Baluteau, J. P., Zavagno, A., Morisett, C., & Péquignot D. 1995, A&A, 303, 175
Barker, T. 1980, ApJ, 240, 99
———. 1982, ApJ, 253, 167
———. 1984, ApJ, 284, 589
———. 1986, ApJ, 308, 314
———. 1987, ApJ, 322, 922
———. 1991, ApJ, 371, 217
Beck, S. C., Lacy, J. H., Townes, C. H., Aller, L. H., Geballe, T. R., & Baas, F. 1981, ApJ, 249, 592
Benvenuti, P., & Perinotto, M. 1981, A&A, 95,127
Bowen, I. S., & Wyse, A. B. 1939, Lick Obs. Bull., 19, 1
Cahn, J., Kaler, J. B., & Stanghellini, L. 1992, A&AS, 94, 399
Capriotti, E. R., Cromwell, R. H., & Williams, R. E. 1971, ApJ, 7, L241
Grevesse, N., & Anders, E. 1989, in Cosmic Abundances in Matter, ed. J. Waddington (New York: AIP), 1
Hajian, A. R., & Terzian, Y. 1996, PASP, 108, 419 (HTz)
Harrington, J. P., Seaton, M. J., Adams, S., & Lutz, J. H. 1982, MNRAS, 199, 517 (HSAL)
Hawley, S. A., & Miller J. S. 1977, ApJ, 212, 94
Hubeny, I. 1988, Comp. Phys. Comm., 52, 103
Hyung, S. 1994, ApJS, 90, 119
Hyung, S., & Aller, L. H. 1996, MNRAS, 278, 551
Kingsburgh, R. L., & Barlow, M. J. 1994, MNRAS, 271, 257
Keenan, F. P., Aller, L. H., Bell, K. L., Hyung, S., McKenna, F. C., & Ramsbottom, C. A. 1996, MNRAS, 281, 1073
Keenan, F. P., Mckenna, F. C., Bell, K. L., Ramsbottom, C. A., Wickstead, W., Aller, L. H., & Hyung, S. 1997, ApJ, 487, 457
Lenzun, P., Natta, A., & Panagia, N. 1989, ApJ, 345, 306
Likkel, L., & Aller, L. H. 1986, ApJ, 301, 825
Middlemass, D., Clegg, R. E. S., Walsh, J. R., & Harrington, J. P. 1991, MNRAS, 251, 284
Moore, C. E. 1974, A Multiplet Table of Astrophys. Interest, National Bureau of Standards, No. 40
———. 1993, in Tables of Spectra of H, C, N, and O, Atoms and Ions, ed. J. W. Gallangher (London: CRC)
Osterbrock, D. E. 1989, Astrophysics of Gaseous Nebulae and Active Galactic Nuclei (Mill Valley: University Science Books)
Osterbrock, D. E., Tran, H. D., & Veilleux, S. 1992, ApJ, 389, 305
Peña, M., & Torres-Peimbert, S. 1981, Rev. Mexicana Astron. Astrophys., 6, 309
Péquignot, D. 1980, A&A, 83, 52
Péquignot, D., & Baluteau, J. P. 1988, A&A, 206, 298
Rowlands, N., Houck, J. R., Herter, T., Gull, G. E., & Seretskie, M. F. 1989, ApJ, 341, 901
Schönberner, D. 1981, A&A, 103, 119
Seaton, M. J. 1979, MNRAS, 187, 73P
Stasinska, G., Tylenda, R., Acker, A., & Stenholm, B. 1992, A&A, 266, 486
Van der Steene, G. C., & Zijlstra, A. A. 1995, A&A, 293, 541
Walker, M. F., & Aller, L. H. 1970, ApJ, 161, 917
Wyse, A. B. 1942, ApJ, 95, 356
Zhang, C. Y. 1995, ApJS, 98, 659